THE JOURNAL OF PHYSICAL CHEMISTRY C

pubs.acs.org/JPCC

Article

Dynamics and Proton Transport in Imidazole-Doped Nanocrystalline Cellulose Revealed by High-Resolution Solid-State Nuclear Magnetic Resonance Spectroscopy

Michał Bielejewski, Monica Pinto-Salazar, Łukasz Lindner, Radosław Pankiewicz, Gerd Buntkowsky, and Jadwiga Tritt-Goc*

Cite This: J. Phys. Chem. C 2020, 124, 18886−18893

Read Online

ACCESS | Metrics & More | Article Recommendations | Supporting Information

ABSTRACT: Imidazole-doped nanocrystalline cellulose (CNC-Im) is a new proton conductor based on imidazole-functionalized nanocrystalline cellulose with a conductivity of approximately 10^{-1} S/m at 160 °C. Its conductivity is possible due to the transport of protons from imidazoles. The dynamics of local processes were studied by ^{15}N and ^{13}C nuclear magnetic resonance (NMR) spectroscopy under the conditions of $^{1}H-^{15}N$ and $^{1}H-^{13}C$ cross-polarization (CP) and magic angle spinning (MAS) and by heteronuclear correlation (HETCOR) spectroscopy. The ^{15}N and ^{13}C NMR spectra showed the coexistence of two fractions of imidazole molecules: slowly reorienting and exchanging protons and fast reorienting and fast exchanging protons. Analysis based on the two-phase model enabled the determination of the energy distribution of imidazole tautomerization, whose maximum value is 38 kJ/mol. The HETCOR experiment allowed determination of the binding of nitrogen protons from imidazoles to cellulose hydroxyl groups and possibly residual water. NMR studies conducted on the ^{13}C isotope confirmed the reorientation of imidazoles. The proton transport in CNC-Im was shown to consist in the exchange of protons between imidazoles via the OH groups of cellulose and residual water conditioned by the reorientation of imidazole rings. The described proton transport leads to the observed conductivity in CNC-Im, assuming the dissociation of imidazole into anion and cation additionally.

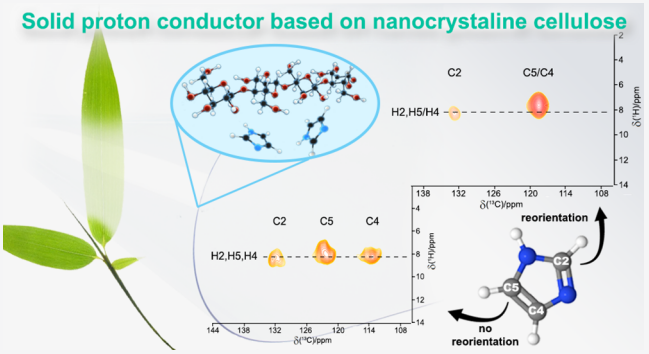

INTRODUCTION

Unfortunately, the destructive impact of man on the environment is already a fact, which is why action is needed to protect this environment from further degradation. The search for new environmentally friendly energy sources is ongoing, and one type of such source is fuel cells.[1−3] The great interest in fuel cells stems from the fact that they are devices that directly convert the energy released in chemical reactions, primarily oxidation of hydrogen, into electricity. As a result, only electricity and water are produced in hydrogen fuel cells. The most important element of a fuel cell that determines its efficiency and durability is the membrane that allows ions to be transported from the anode to the cathode. The membrane should be an electron nonconductive material and should act as a gas separation barrier (H_2 and O_2). It has to be mechanically, chemically, and thermally stable, and inexpensive. There are different types of fuel cells, including the proton exchange membrane fuel cells (PEMFC),[4] which are of particular interest as the most promising for transport applications. Today, mainly perfluorinated polymers containing sulfonic groups such as Nafion, Aciplex, and Flemion are competitive for use in PEMFC systems.[5] However, all of them are expensive in production and limited to low-temperature operation. The latter limitation is related to the fact that the proton transport in these membranes is based on the diffusion of water as proton-carrying molecules (vehicle mechanism) and depends on the degree of membrane hydration. For example, Nafion conductivity is in the range between 1 and 21.5 S/m,[6] depending on the water content, and hence its use is limited to approximately 100 °C. For technological reasons, it is desirable to produce proton conductive membranes that can work at higher temperatures, because PEMFC operating in such conditions improves the tolerance of the Pt electrode for carbon monoxide, provides higher efficiency, and has easier heat management. There are various ways to increase the operating temperature while maintaining proton conductivity.

Received: May 31, 2020
Revised: August 7, 2020
Published: August 10, 2020

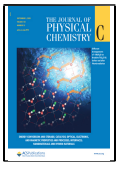

One of the ideas is to replace water with other proton carriers such as amphoteric nitrogen-based heterocycles, which can act as both proton accepters and donors within a dynamical hydrogen-bond network.[7] Heterocycles attached to a polymer backbone serve as solid proton solvent, which does not evaporate from the fuel cell under high temperature, unlike water in the classic Nafion and other acid functionalized polymers. The conductivity of protons in such anhydrous proton conductive membranes with heterocycles usually occurs via the Grotthuss mechanism, where only the protons are mobile and jump from a protonated nitrogen of a heterocyclic molecule to nonprotonated nitrogen in an adjacent heterocyclic molecule. The proton transfer also includes continuous breaking and reformation of the hydrogen-bond network involving the heterocycles and their reorientation.[8] It is worth noting that the melting point of nitrogen-based heterocyclic molecules is approximately 200 °C, meaning that the working temperature of up to 150 °C is still lower than the melting point, and the proton transfer takes place in a solid state. Therefore, polymer electrolyte membranes with heterocycles are possible alternative materials for membrane functioning >100 °C. Most of them are based on synthetic polymers, which makes them expensive and not environmentally friendly.[9−16] To eliminate these drawbacks, we proposed to use cellulose as a host polymer. Membranes composed of imidazole-doped microcrystalline cellulose (CMC-Im), imidazole-doped nanocrystalline cellulose (CNC-Im), and triazole-doped nanocrystalline cellulose (CNC-Tri) have been synthesized and have been the subject of our extensive studies. We focused on their thermal and conductivity properties, and also on the dynamics.[17−22] The CMC-Im with the highest concentration of Im showed the conductivity of 2.0×10^{-4} S/m at 160 °C whereas,[17] at the same temperature, CNC-Im showed the highest conductivity of 4.0×10^{-1} S/m.[19] In both cases, the conductivity was measured under anhydrous conditions. It depends mainly on the efficiency of proton transport based on local processes at the molecular level involving the temporary localization at the specific binding size of the protons as well as their hopping between these binding sites and the rotational speed of heterocycle.

Solid-state nuclear magnetic resonance (NMR) spectroscopy under fast magic angle spinning (MAS) is a unique method to study the local molecular mobility and dynamics processes.[23] That is why we used this method to answer the question of what is the proton transport mechanism that determines the mechanism of conductivity in CMC-Im. The data obtained from solid-state ^{15}N NMR techniques at variable temperature allowed us to postulate the Grotthuss mechanism.[20] The protons are transferred within the hydrogen-bond network from one imidazole (Im) ring to the other via hydroxyl groups of cellulose or residual water. Im generates protonic charge carriers by self-dissociation. Proton transfer is coupled to hydrogen-bond breaking and forming processes.

We hypothesized that the same proton transport mechanism occurs in CNC-Im. To test this hypothesis, we performed the high-resolution solid-state NMR to study the local mobility in CNC-Im. Variable temperature experiments ^{15}N and ^{13}C NMR under conditions of ^{1}H−^{15}N and ^{1}H−^{13}C cross-polarization (CP) and MAS were especially suitable to study the exchange of protons and reorientation of Im. The ^{1}H−^{15}N HETCOR experiment allowed determination of which protons of the composite are exchanged with the Im protons, and ^{1}H−^{13}C HETCOR proved the dynamics of Im. In this paper, we report a series of experimental findings whose interpretation provides information on the microscopic processes that give rise to proton transport in the CNC-Im. Understanding the molecular aspects of CNC-Im proton conduction, in particular, the relationship between molecular dynamics and conductivity is a key point to achieve proton transport with high-efficiency in such cellulose-based materials.

One of the research goals of this work was also to find out whether the replacement of microcrystalline cellulose with its nanocrystalline form as a polymer host in the composite affects the dynamics of local processes. At 160 °C, the conductivity of the CNC-Im is three orders of magnitude higher than CMC-Im. This result can be explained taking into account that nanocrystalline cellulose retains all cellulose properties, including the distribution of −OH groups along polymer chains that can be functionalized with Im, but additionally, it is characterized by a very large surface area.[24] The latter feature allowed more effective functionalization of nanocrystalline cellulose with Im than that of microcrystalline cellulose. The higher concentration of Im in CNC-Im is one of the factors, which lead to higher conductivity. In this article, we show that another factor, namely the dynamics of local processes, can also positively affect the conductivity of this composite. On the basis of the ^{15}N CPMAS experiment performed as a function of temperature, it was found that the exchange of Im protons in CNC-Im begins at a lower temperature and with lower activation energy compared to those of CMC-Im.

Although there are many reports on heterocycles-containing polymers in PEMFC, most of them deal with the study of material properties and their conductivity. The dynamics of local processes have rarely been studied, and the conductivity mechanism is often presumed without the experimental basis that NMR measurements provide. This work focuses on the dynamics of Im, which acts as a proton solvent in a composite based on nanocrystalline cellulose functionalized with Im. CNC-Im can be considered for potential applications as a solid electrolyte in fuel cells.

EXPERIMENTAL SECTION

Materials. Nanocrystalline cellulose desulfated (CNC) was purchased from the Cellulose Lab from Canada as a stable suspension of nanocrystals at a concentration of 8% by weight. The CNC crystallinity index was 78%, the crystal length was 140−200 nm, and the crystal width was 5−20 nm. To functionalize cellulose, Imenriched in ^{15}N isotope, 98% pure, was purchased from the Sigma-Aldrich company. The CNC-Im composite was synthesized by the method described in reference[19] and obtained in the form of a colorless, transparent film with a thickness of 0.234 mm. On the basis of elemental analysis, the molar ratio of glucose units to Im is equal to 1.3.[19] The initial water content of CNC-Im sample is approximately 5% (wt %).[21]

^{1}H−^{15}N CPMAS and ^{1}H−^{15}N HETCOR CPMAS Spectroscopy. ^{1}H−^{15}N CPMAS measurements were taken at the Technical University of Darmstadt on a 14.1 T Bruker Avance III HD spectrometer at 60.82 MHz ^{15}N Larmor frequency. A 4 mm probe and an MAS frequency of 7.5 kHz was used in the experiments. The recycle delay, contact time, and the decoupling field were set to 10 s, 3.5 ms, and 80 kHz, respectively. The spectra were recorded using 512 scans.

The 2D ^{1}H−^{15}N heteronuclear correlation (HETCOR) experiments were carried out at the Institute of Molecular Physics PAS in Poznan an 11.7 T Bruker Avance III HD

https://dx.doi.org/10.1021/acs.jpcc.0c04905
J. Phys. Chem. C 2020, 124, 18886−18893

spectrometer operating at ^{15}N Larmor frequency of 50.68 MHz. The measurements were performed with the use of the frequency switched Lee−Goldburg decoupling at a spinning rate of 7.5 kHz.[25] To eliminate coupling to remote protons, two contact times were used: 0.6 and 1.2 ms. The extended contact time did not cause any significant change in the spectra except for a better signal-to-noise ratio (S/N) ratio. The ^{1}H homonuclear decoupling was achieved by using the FSLG pulse sequence with a transverse ^{1}H field strength of 100 kHz.[26]

$^{1}H-^{13}C$ CPMAS and $^{1}H-^{13}C$ HETCOR CPMAS Spectroscopy. $^{1}H-^{13}C$ CPMAS experiments were carried out on an 11.7 T Bruker Avance III HD spectrometer operating at ^{13}C Larmor frequency of 125.76 MHz and located at the Institute of Molecular Physics PAS in Poznan. The resonance probe with 4 mm MAS rotors spinning of 10 kHz was used. All CPMAS spectra were recorded with 1.2 ms contact time and using a recycle delay of 5 s. The decoupling field was set to 75 kHz, and 2048−4096 scans were made.

2D $^{1}H-$- ^{13}C HETCOR experiments were performed with the use of the frequency-switched Lee-Goldburg decoupling (FSLG) sequence[26] and MAS spinning rate of 10 kHz. The FSLG pulse sequence with a transverse ^{1}H field strength of 83 kHz was used for homonuclear ^{1}H decoupling.[27] The experiments were performed with two contact times, 0.6 and 1.2 ms. Increasing the contact time did not cause any significant changes in the recorded spectra, but provided a better S/N. All ^{15}N and ^{13}C spectra reported here were measured as a function of temperature from 233 to 353 K. A given temperature was stabilized for 15 min before the measurements, and the temperature step was equal to 5 K. The spectra were referenced to glycine (33.4 ppm, ^{15}N and 176 ppm, ^{13}C).[27,28]

The experiments were performed on ^{15}N-labeled Im and ^{13}C natural abundance Im embedded in nanocrystal cellulose.

RESULTS AND DISCUSSION

The ^{15}N and ^{13}C CPMAS NMR spectra of CNC-Im, measured as a function of temperature, provide us with information on the molecular motions of the Im molecules and their tautomerism. The 2D $^{1}H-^{15}N$ HETCOR spectra indicate the hydrogen bonds of Im protons, and thus possible proton exchange sites. The 2D $^{1}H-^{13}C$ HETCOR spectra revealed the reorientation of the Im ring.

$^{1}H-^{15}N$ CPMAS NMR Spectra of CNC-Im^{15}N. Cellulose is formed by one type of repeat glucose unit, but in CNC-Im, some of them are hydrogen-bonded to Im, whereas the others not. Moreover, Im can be bonded directly to hydroxyl groups of cellulose or indirectly through residual water molecules but only on the cellulose surfaces.[17,20] Therefore, CNC-Im, like other composites, is a disordered system and can be characterized by the distribution of microenvironments, which differently modify the dynamics (reorientation) of the Im molecules and affect the NMR signal. Motional heterogeneities can be described in terms of a distribution of correlation times or tautomerization rate constants.[20,29−33] Assuming a broad distribution of these parameters at low temperature, the NMR spectrum can be approximated by a superposition of only two spectra corresponding to very slow or very fast exchanging protons and reorienting molecules, neglecting the spectra of the intermediate regime. Such a case is called the two-phase model.[31−34] The subspectrum corresponding to mobile molecules disappears at very low temperature and only the spectrum corresponding to the rigid molecules remains. Analysis of the temperature dependence of the line shape obtained based on this model directly gives the shape of activation energy distribution for a given matrix.

Figure 1 shows a series of selected ^{15}N CPMAS NMR spectra acquired between 243 and 343 K thus, well below the

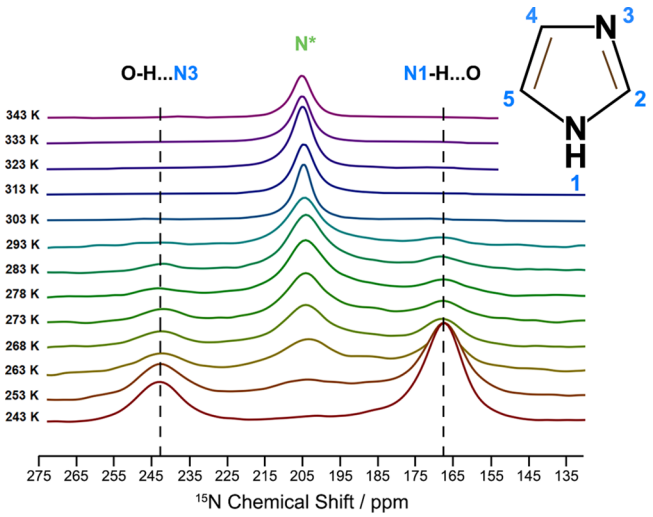

Figure 1. Selected $^{1}H-^{15}N$ CPMAS NMR spectra of CNC-Im-^{15}N measured at 14.1 T and a spinning rate of 7.5 kHz, at different temperature.

Im melting point at 364 K. At the lowest temperature, a typical ^{15}N spectrum of Im is observed with two separate high-field amino (N1) and the low-field imino (N3) nitrogens signals with rotational sidebands as shown in Figure S1. Such spectrum corresponds to rigid Im molecules slowly exchanging protons. At the highest temperature, only a liquid-like sharp coalesced signal located exactly in the center between imino and amino signals of rigid Im is observed without rotational sidebands (see Figure S1). This signal corresponds to fast exchanging Im amino/imino nitrogens. The absence of the rotational sidebands indicates that the tautomerism is coupled with a rapid reorientation of Im. Between 253 and 293 K, the so-called two-phase spectra are observed being a superposition of spectra described above. With increasing the temperature the intensity of the lines corresponding to slowly exchanging rigid molecules decreases and the intensity of the rapidly exchanging and reorienting molecules increases as seen in Figure 1.

The two-phase spectra observed in Figure 1 reveal a distribution of Im tautomerization rate constants arising from a structural heterogeneity of CNC-Im. The relative concentration of the two phases can be written as a shifted Gauss error-function:[31]

$$C_A(T) = \frac{1}{2}\mathrm{erf}\left(\frac{1}{\sqrt{2}\,\Delta T}(T - T_0)\right) + \frac{1}{2}\mathrm{erf}\left(\frac{1}{\sqrt{2}\,\Delta T}T_0\right)$$
$$C_B(T) = 1 - C_B(T) \quad (1)$$

where C_A and C_B are the fraction of the spectrum corresponding to fast and slow exchanging protons Im molecules, respectively, and $\mathrm{erf}(x)$ is the Gaussian error function. The function given by eq 1 is zero at low temperature and one at high temperature. T_0 defines the temperature where

https://dx.doi.org/10.1021/acs.jpcc.0c04905
J. Phys. Chem. C 2020, 124, 18886−18893

both fractions are 0.5. ΔT describes the temperature range of the transition from slow to fast exchange spectra. The distribution of activation energy in temperature units can be determined by differentiation eq 1 with respect to temperature:

$$g(T) = \frac{\mathrm{d}}{\mathrm{d}T}C_A(T) = \frac{1}{\sqrt{2}\pi\Delta T}\exp\left(-\frac{(T-T_0)^2}{2\Delta T^2}\right) \quad (2)$$

Equation 2 can be converted into the distribution of activation energy by assuming an Arrhenius dependence between the activation energy, temperature, and the exchange rate constant.

We used the two-phase model to describe the temperature dependence of ^{15}N NMR spectra presented in Figure 1. In this model, the relative intensities of the lines are proportional to the relative concentration of the two phases. Figure 2a shows

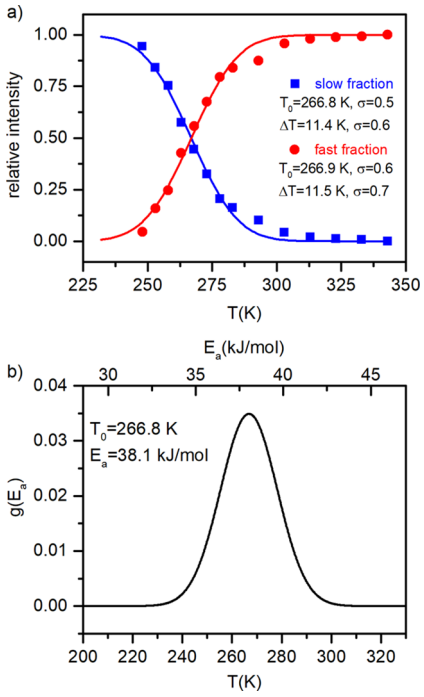

Figure 2. (a) Relative concentration of imidazole fractions of slowly and fast exchanging protons in CNC-Im-^{15}N. The lines are the best fits of eq 1 to the points derived from the spectra as shown in Figure 1. (b) Distribution of the activation energy of proton tautomerism of imidazole in CNC-Im.

the fraction of the Im molecules corresponding to both phases. As can be seen, the fraction of the slowly exchanging rigid molecules decreases with increasing temperature, whereas the fraction of the rapidly exchanging and reorienting molecules increases. The solid lines shown in Figure 2 are the results of the best fits of eq 1 to the points derived from the experimental spectra shown in Figure 1. The best-fitting parameters are the center-temperature T_0 = (266.8 ± 0.4) K and the temperature width ΔT = (11.5 ± 0.5) K. On the basis of eq 2 and the values of fitted parameters, the activation energy distribution of the proton tautomerism of Im in CNC-Im was calculated, and the resulting curve is shown in Figure 2b. The distribution function is symmetric with a full width at half-height of 4 kJ/mol. The main activation energy is E_a = 38.1 kJ/mol.

It is interesting to compare the values of the above parameters with those evaluated for CMC-Im composite for which T_0 = 293.6 K, ΔT = 24.7 K, E_a = 42 kJ/mol and a full width at half-height of the distribution function is 9 kJ/mol.[20] The following conclusion can be drawn. In CNC-Im, the temperature range of the transition from slow to fast exchange spectra ΔT, (Figure 2a) is about two times narrower, and the temperature T_0 is reduced by 26 K as compared to the previously studied CMC-Im composite. In CNC-Im, also a narrower distribution of energies of activation of the Im tautomerization, $g(E_a)$, and lower value at maximum by 4 kJ/mol is obtained, compared to CMC-Im. The above facts indicate that in CNC-Im, the reorientation of imidazoles and the exchange of protons begin at a lower temperature and with lower activation energy than in CMC-Im. Because the activation energy distribution reflects the homogeneity of the composite, we can also conclude that CNC-Im is a more ordered system than CMC-Im.

2D ^{1}H−^{15}N HETCOR Spectroscopy of CNC-Im ^{15}N. The 2D ^{1}H−^{15}N HETCOR NMR correlation experiment was performed at 308 and 238 K. Figure 3 shows the relevant

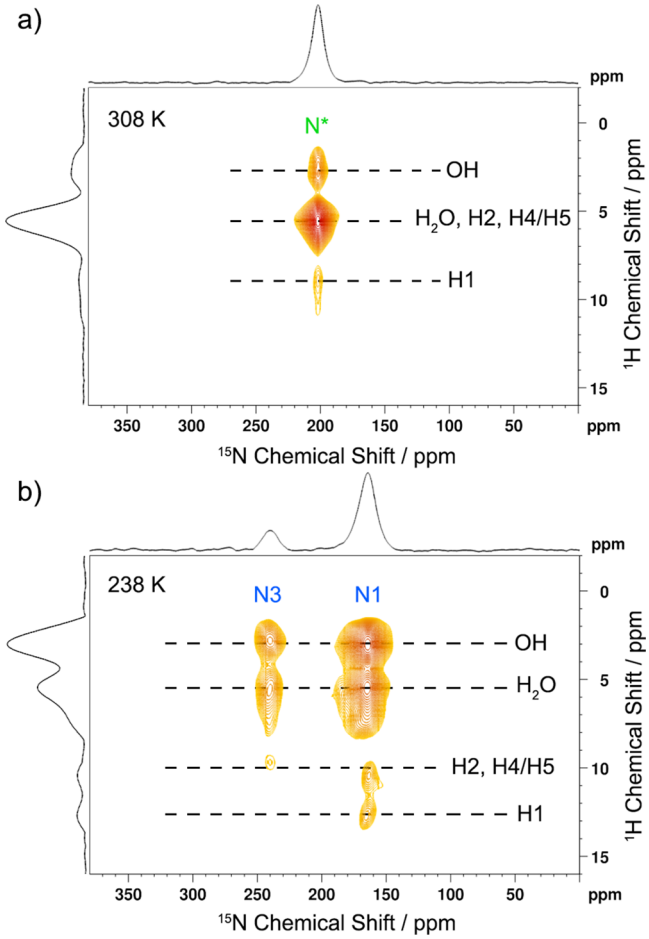

Figure 3. 2D ^{1}H−^{15}N HETCOR NMR spectra of CNC-Im-^{15}N recorded at 308 K (a), and 238 K (b), at 11.74 T

spectra. The 1D projection of the HETCOR spectrum at 238 K into the ^{1}H dimension shows a strong high-field peak around 3 ppm assigned to OH groups of cellulose followed by a signal around 5 ppm assigned to OH-groups of water. The signals observed approximately 10 and 12 ppm were assigned to the aromatic hydrogens of imidazole (H2, H4/H5) and amino (H1) protons based on the 263 K ^{1}H−^{15}N HETCOR

https://dx.doi.org/10.1021/acs.jpcc.0c04905
J. Phys. Chem. C 2020, 124, 18886−18893

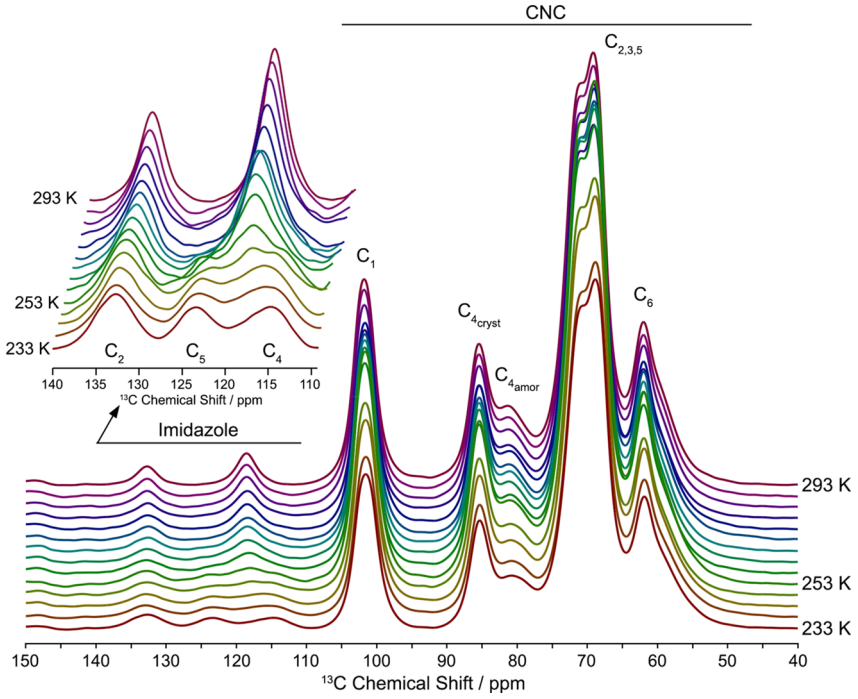

Figure 4. Selected $^{1}H-^{13}C$ CPMAS NMR spectra of CNC-Im measured at 11.7 T and a spinning rate of 10 kHz, at different temperatures. The insert shows only the spectra of imidazole carbons.

spectrum of ^{15}N imidazole.[20] The 1D projection of the 308 K spectrum into the ^{15}N dimension gives the spectrum corresponding to the rigid imidazole molecules and thus, with two signals of chemically nonequivalent nitrogen atoms (N1 and N3). At 308 K, the projection of the spectrum into the ^{15}N dimension gives only one signal at 200 ppm corresponding to the fast exchanging imidazole amino/imino nitrogens. The projection into the ^{1}H dimension (Figure 3a) shows two peaks around 3 and 5 ppm, which were assigned to OH-groups of cellulose and H_2O, respectively. In this spectrum, the intensity of the signals is opposite as in the spectrum at 238 K. This is because now the signal at 5 ppm corresponds not only to the fast exchanging NH-protons of imidazole and OH-groups of water but also to the aromatic imidazole protons. The observed peak is the superposition of these two peaks.

The results presented in Figure 3 indicate that imidazoles form hydrogen bonds with hydroxyl groups of nanocrystalline cellulose and water molecules and that their tautomerization in CNC-Im is coupled to proton exchange with protons of these groups.

$^{1}H-^{13}C$ CPMAS NMR Spectra of CNC-Im. Additional evidence that CNC-Im comprises two dynamically nonequivalent imidazole molecules (rigid and fast rotating molecules) was obtained from the NMR spectra on ^{13}C in natural abundance. The ^{13}C CPMAS spectra were measured in the temperature range from 233 to 353 K and in a wide range of frequencies from 40 to 150 ppm. Therefore, they contained the spectrum of Im (110 and 150 ppm) but also that of nanocrystalline cellulose (40 to 110 ppm), as shown in Figure 4. The latter spectrum is similar to the spectra of cellulose and cellulose-containing materials previously reported, and the assignment to cellulose carbons is standard as shown in Figure 4.[35] The ^{13}C spectra of Im are presented in more detail in the insert in Figure 4.

The spectrum at 233 K is typical of the rigid Im molecule, and it contains three signals: two from chemically nonequivalent Im carbons C4 and C5 in basal position observed at 116 and 126 ppm, respectively, and the apical resonance (carbon C2) at a 134 ppm. The spectrum at the highest temperature contains only a single resonance line located between the C4 and C5 resonances of rigid molecules. This line corresponds to rapidly exchanging protons and reorienting Im molecules. Between these temperatures in the CNC-Im, in contrast to the temperature-dependent coalescence process of basal ^{13}C resonances in the ordered system,[36] the two-phase ^{13}C spectra are observed, best visible at 250 K.

The intensity of the ^{13}C resonances of rigid Im 's at 233 K decreases with increasing temperature at the expense of increasing the intensity of the signal assigned to the rapidly exchanging protons and fast reorienting Im's.

Generally, Im reorientation averages the orientation-dependent dipolar couplings and heterogeneous distribution of chemical shifts resulting from various local packing arrangements in disordered CNC-Im. Both phenomena cause a reduction of the line width with increasing temperature and thus increasing molecular mobility. Such temperature behavior was observed for the resonances assigned to the carbons of Im molecules (Figure 5). The line widths of all resonances were obtained by fitting the appropriate number of Gaussian and/or Lorentzian lines to experimental spectra. The line width of Im ^{13}C resonances decreases with increasing temperature for both phases but with a different character of temperature dependence. The centerline corresponding to the fast exchanging protons and reorienting Im molecules shows a continuous, almost linear line narrowing with increasing temperature (Figure 5b). This shows that the exchange process and mobility of the ring are constantly increasing. Interesting behavior is noted for the temperature dependence of the line width of the rigid Im molecule (Figure 5a). In the range from

https://dx.doi.org/10.1021/acs.jpcc.0c04905
J. Phys. Chem. C 2020, 124, 18886−18893

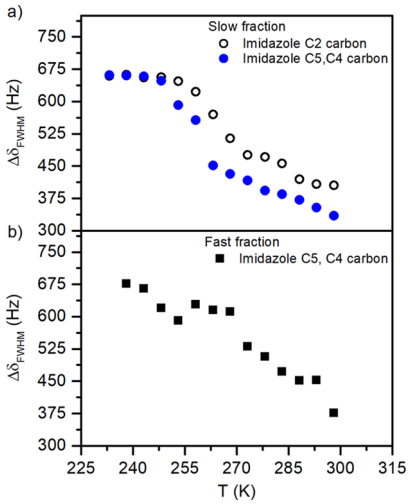

Figure 5. Changes in line width of carbon resonances at different temperatures (a) for slow reorienting and (b) fast reorienting Im molecules in CNC-Im. Points were obtained from the spectra in Figure 4 in the fitting procedure.

233 to 250 K, a plateau value is observed followed by a continuous line narrowing with increasing temperature. A most pronounced decrease in the line narrowing of ^{13}C NMR signals is observed between 250 and 265 K. This temperature range almost exactly matches the temperature interval in which the transition from slow to fast exchange spectra takes place, as follows from the ^{15}N CPMAS spectra of CNC-Im. This fact proves that the ring reorientation is closely linked to the proton exchange in CNC-Im.

The question arises whether Im's in CNC-Im perform reorientations around the C_2 axis of the ring as in the model Im compound such as imidazolium methyl sulfonate.[36] Reorientation around C_2 averages the basal $^1H-^{13}C$ dipolar interactions, whereas it does not or only negligibly averages the apical $^1H-^{13}C$ dipolar coupling, leaving the line width of the apical carbon unchanged as a function of temperature. Undoubtedly, the analysis of ^{13}C CPMAS line width testifies to the reorientation of the Im ring in CNC-Im. The evidence of the same influence of temperature on apical, C2, and basal resonances, C4, C5, given in Figure 5a may suggest that the reorientation of Im in CNC-Im does not occur around the C_2 axis. However, given that the spectra were measured at high-power proton decoupling and MAS, the C2 axis reorientation model cannot be excluded.

The spectra assigned to nanocrystalline cellulose showed almost no evidence of change over the temperature range studied. The line widths of the signal assigned to C_1 is almost constant in the temperature range from 233 to 300 K. This behavior indicates that the host polymer in CNC-Im is characterized by a very low degree of mobility.

2D $^1H-^{13}C$ HETCOR Spectroscopy of CNC-Im. 2D $^1H-^{13}C$ HETCOR spectra confirmed the dynamics of Im in CNC-Im composite (Figure 6). At 233 K, all molecules are rigid, and a characteristic 2D spectrum of Im carbons is observed. However, at T = 255 K two separate resonances for C4 and C5 carbons are not observed. In the composite, at this temperature, besides the rigid molecules, there are also the reorienting molecules and the observed 2D spectrum is a superposition of the spectra corresponding to rigid and fast reorienting Im's. The dynamics of molecules of both fractions

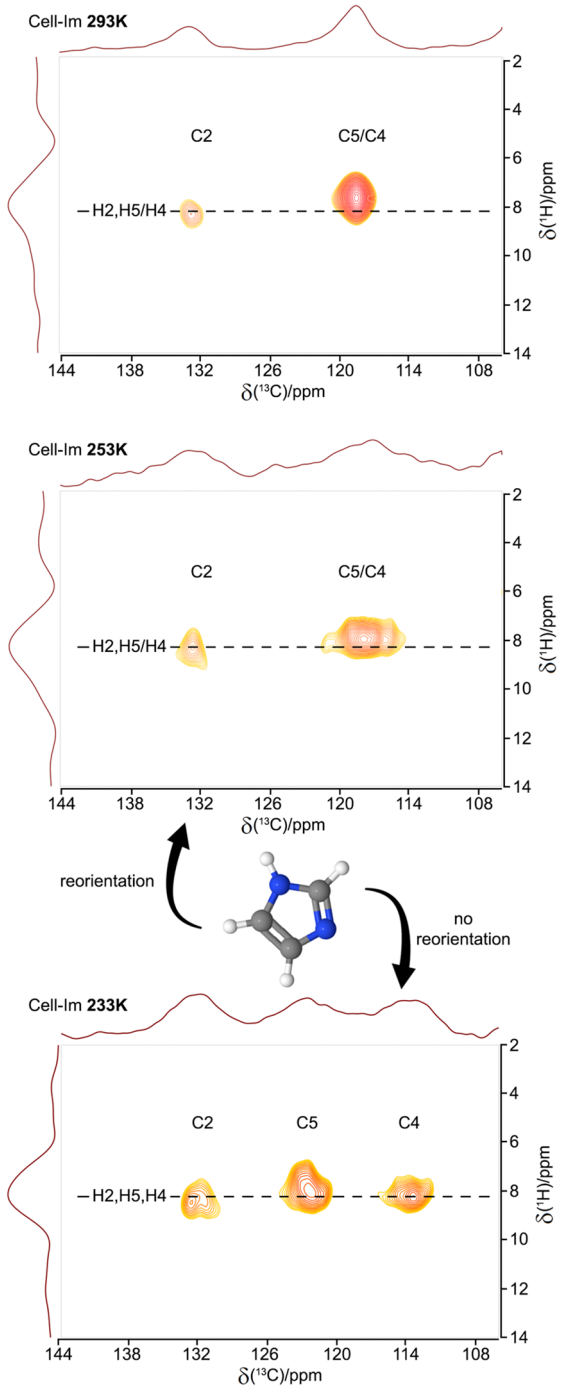

Figure 6. 2D $^1H-^{13}C$ HETCOR NMR spectra of CNC-Im- recorded at 11.7 T as a function of temperature. Only ^{13}C spectra of imidazoles are shown in the figure.

increase as a function of temperature, which is manifested in the 2D spectra shown in Figure 6.

CONCLUSIONS

The results presented in this paper were obtained by the solid-state high-resolution NMR methods. The subject of the research was the composite based on Im-functionalized nanocrystalline cellulose, CNC-Im, which has a proton conductivity of 10^{-1} S/m at 160 °C and thus could be potentially used as a membrane material for fuel cells. The studies were performed on ^{15}N and ^{13}C isotopes and

https://dx.doi.org/10.1021/acs.jpcc.0c04905
J. Phys. Chem. C 2020, 124, 18886−18893

concerned local dynamic processes enabling proton transport in the composite, responsible for conductivity. ^{15}N CPMAS spectra as a function of temperature were interpreted using the two-phase model. In a given temperature range, the spectra of nitrogen from imidazoles are spectral superpositions of rigid slow-exchanging and of fast reorienting and exchanging protons. On the basis of the two-phase model, the tautomerization energies of imidazoles in the CNC-Im were calculated. By using 2D $^{1}H-^{15}N$ HETCOR, we have shown that only the protons at the Im nitrogen in CNC-Im bind with cellulose OH groups as well as with residual water.

The temperature-dependent changes in the ^{13}C CPMAS and the $^{1}H-^{13}C$ HETCOR spectra confirmed the mobility of Im rings.

The obtained results proved that in the CNC-Im nanocomposite, as in the previously studied CMC-Im composite, proton transport consists of their exchange between neighboring imidazoles but via OH groups of cellulose and possibly water. The reorientation of imidazolium rings is a condition enabling the exchange process and activating the dynamics of the hydrogen-bond network in which imidazoles, OH groups of cellulose, or residual water participate. The described process of proton transport is responsible for conductivity in CNC-Im assuming that the process of reorganization of hydrogen bonds and proton exchange is accompanied by dissociation of imidazole into anions and cations. The proton transport mechanism and proton conductivity mechanism in CNC-Im are therefore the same as in CMC-Im. Replacement of microcrystalline cellulose with nanocrystalline resulted in an increase in conductivity by three orders of magnitude, which cannot result only from the greater efficiency of functionalization of nanocrystalline cellulose with Im but, as shown in the paper, also from greater mobility of Im in the CNC-Im nanocomposite than in CMC-Im.

■ ASSOCIATED CONTENT

Supporting Information

The Supporting Information is available free of charge at https://pubs.acs.org/doi/10.1021/acs.jpcc.0c04905.

Selected ^{15}N CPMAS NMR spectra of CNC-Im-^{15}N with amino and imino sidebands (PDF)

■ AUTHOR INFORMATION

Corresponding Author

Jadwiga Tritt-Goc − *Institute of Molecular Physics Polish Academy of Sciences, 60-179 Poznań, Poland;* orcid.org/0000-0003-3994-284X; Phone: +48-61 8695-226; Email: jtg@ifmpan.poznan.pl; Fax: +48 61 8684524

Authors

Michał Bielejewski − *Institute of Molecular Physics Polish Academy of Sciences, 60-179 Poznań, Poland*

Monica Pinto-Salazar − *Institute of Inorganic and Physical Chemistry, Technical University of Darmstadt, D-64287 Darmstadt, Germany*

Łukasz Lindner − *Institute of Molecular Physics Polish Academy of Sciences, 60-179 Poznań, Poland;* orcid.org/0000-0002-5187-6008

Radosław Pankiewicz − *Faculty of Chemistry, Adam Mickiewicz University in Poznań, 61-614 Poznań, Poland*

Gerd Buntkowsky − *Institute of Inorganic and Physical Chemistry, Technical University of Darmstadt, D-64287 Darmstadt, Germany;* orcid.org/0000-0003-1304-9762

Complete contact information is available at: https://pubs.acs.org/10.1021/acs.jpcc.0c04905

Notes

The authors declare no competing financial interest.

■ ACKNOWLEDGMENTS

This work was supported by the National Science Centre Poland [grant number 2017/25/B/ST8/00973 to JTG, MB, and ŁL]. MB thanks Prof. G. Buntkowsky for staying in the laboratory and learning NMR experiments on high-resolution solid-state NMR in Darmstadt. His stay was financed from the grant mention above. GB and MP thank the Deutsche Forschungsgemeinschaft for financial support under contract Bu-911-26-1. MB and MP thank Dr. Pedro Groszewicz for initial help in setting up the 14 Tesla NMR experiments.

■ REFERENCES

(1) Arshad, A.; Ali, H. M.; Habib, A.; Bashir, M. A.; Jabbal, M.; Yan, Y. Energy and exergy analysis of fuel cells: A review. *Therm. Sci. Eng. Prog.* **2019**, *9*, 308−321.

(2) Wang, S.; Jiang, S. P. Prospects of fuel cell technologies. *Natl. Sci. Rev.* **2017**, *4*, 163−166.

(3) Sharaf, O. Z.; Orhan, M. F. An overview of fuel cell technology: Fundamentals and applications. *Renew. Sustainable Energy Rev.* **2014**, *32*, 810−853.

(4) Yonoff, R. E.; Ochoa, G. V.; Cardenas-Escorcia, Y.; Silva-Ortega, J. I.; Meriño-Stand, L. Research trends in proton exchange membrane fuel cells during 2008 − 2018: A bibliometric analysis. *Heliyon* **2019**, *5*, No. e01724.

(5) Kusoglu, A.; Weber, A. Z. New insights into perfluorinated sulfonic-acid ionomers. *Chem. Rev.* **2017**, *117*, 987−1104.

(6) Zhao, J.; Li, X. A review of polymer electrolyte membrane fuel cell durability for vehicular applications: Degradation modes and experimental techniques. *Energy Convers. Manage.* **2020**, *199*, 112022.

(7) Kreuer, K. D. Proton conductivity: Materials and applications. *Chem. Mater.* **1996**, *8*, 610−641.

(8) Münch, W.; Kreuer, K.-D.; Silvestri, W.; Maier, J.; Seifert, G. The diffusion mechanism of an excess proton in imidazole molecule chains: first results of an ab initio molecular dynamics study. *Solid State Ionics* **2001**, *145*, 437−443.

(9) Akbey, Ü.; Granados-Focil, S.; Coughlin, E. B.; Graf, R.; Spiess, H. W. ^{1}H solid-state NMR investigation of structure and dynamics of anhydrous proton conducting triazole-functionalized siloxane polymers. *J. Phys. Chem. B* **2009**, *113*, 9151−9160.

(10) Bozkurt, A.; Meyer, W. H.; Wegner, G. PAA/imidazol-based proton conducting polymer electrolytes. *J. Power Sources* **2003**, *123*, 126−131.

(11) Yamada, M.; Honma, I. Anhydrous protonic conductivity of a self-assembled acid-base composite material. *J. Phys. Chem. B* **2004**, *108*, 5522−5526.

(12) Yamada, M.; Honma, I. Alginic acid − imidazole composite material as anhydrous proton conducting membrane. *Polymer* **2004**, *45*, 8349−8354.

(13) Yamada, M.; Honma, I. Anhydrous proton conducting polymer electrolytes based on poly(vinylphosphonic acid)-heterocycle composite material. *Polymer* **2005**, *46*, 2986−2992.

(14) Pangon, A.; Totsatitpaisan, P.; Eiamlamai, P.; Hasegawa, K.; Yamasaki, M.; Tashiro, K.; Chirachanchai, S. Systematic studies on benzimidazole derivatives: Molecular structures and their hydrogen bond networks formation toward proton transfer efficiency. *J. Power Sources* **2011**, *196*, 6144−6152.

(15) Goward, G. R.; Schuster, M. F. H.; Sebastiani, D.; Schnell, I.; Spiess, H. W. High-resolution solid-state NMR studies of imidazole-based proton conductors: Structure motifs and chemical exchange from ^{1}H NMR. *J. Phys. Chem. B* **2002**, *106*, 9322−9334.
(16) Benhabbour, S. R.; Chapman, R. P.; Scharfenberger, G.; Meyer, W. H.; Goward, G. R. Study of imidazole-based proton-conducting composite materials using solid-state NMR. *Chem. Mater.* **2005**, *17*, 1605−1612.
(17) Smolarkiewicz, I.; Rachocki, A.; Pogorzelec-Glaser, K.; Pankiewicz, R.; Ławniczak, P.; Łapiński, A.; Jarek, M.; Tritt-Goc, J. Proton-conducting microcrystalline cellulose doped with imidazole. Thermal and electrical properties. *Electrochim. Acta* **2015**, *155*, 38−44.
(18) Tritt-Goc, J.; Jankowska, I.; Pogorzelec-Glaser, K.; Pankiewicz, R.; Ławniczak, P. Imidazole-doped nanocrystalline cellulose solid proton conductor: synthesis, thermal properties, and conductivity. *Cellulose* **2018**, *25*, 281−291.
(19) Tritt-Goc, J.; Lindner, Ł.; Bielejewski, M.; Markiewicz, E.; Pankiewicz, R. Proton conductivity and proton dynamics in nanocrystalline cellulose functionalized with imidazole. *Carbohydr. Polym.* **2019**, *225*, 115196.
(20) Zhao, L.; Smolarkiewicz, I.; Limbach, H.-H.; Breitzke, H.; Pogorzelec-Glaser, K.; Pankiewicz, R.; Tritt-Goc, J.; Gutmann, T.; Buntkowsky, G. Buntkowsky, G, Imidazole-doped cellulose as membrane for fuel cells: Structural and dynamic insights from solid-state NMR. *J. Phys. Chem. C* **2016**, *120*, 19574−19585.
(21) Bielejewski, M.; Lindner, Ł.; Pankiewicz, R.; Tritt-Goc, J. The kinetics of thermal processes in imidazole-doped nanocrystalline cellulose solid proton conductor. *Cellulose* **2019**, *27*, 1989−2001.
(22) Tritt-Goc, J.; Lindner, Ł.; Bielejewski, M.; Markiewicz, E.; Pankiewicz, R. Synthesis, thermal properties, conductivity and lifetime of proton conductors based on nanocrystalline cellulose surface-functionalized with triazole and imidazole. *Int. J. Hydrogen Energy* **2020**, *45*, 13365−13375.
(23) Hansen, M. R.; Graf, R.; Spiess, H. W. Interplay of structure and dynamics in functional macromolecular and supramolecular systems as revealed by Magnetic Resonance Spectroscopy. *Chem. Rev.* **2016**, *116*, 1272−1308.
(24) Trache, D.; Hussin, M. H.; Haafiz, M. K. M.; Thakur, V. K. Recent progress in cellulose nanocrystals: sources and production. *Nanoscale* **2017**, *9*, 1763−1786.
(25) Lee, M.; Goldburg, W. I. Nuclear-Magnetic-Resonance line narrowing by a rotating rf field. *Phys. Rev.* **1965**, *140*, 1261−1271.
(26) Bielecki, A.; Kolbert, A. C.; Levitt, M. H. Frequency-switched pulse sequences: homonuclear decoupling and dilute spin NMR in solids. *Chem. Phys. Lett.* **1989**, *155*, 341−346.
(27) Taylor, R. E. ^{13}C CP/MAS: Application to glycine. *Concepts Magn. Reson. Part A Bridg. Educ. Res.* **2004**, *22A*, 79−89.
(28) Bertani, P.; Raya, J.; Bechinger, B. ^{15}N chemical shift referencing in solid state NMR. *Solid State Nucl. Magn. Reson.* **2014**, *61-62*, 15−18.
(29) Schmidt, C.; Kuhn, K. J.; Spiess, H. W. Distribution of correlation times in glassy polymers from pulsed deuteron NMR. *Prog. Colloid Polym. Sci.* **1985**, *71*, 71−76.
(30) Wehrle, M.; Hellmann, G. P.; Spiess, H. W. Phenylene motion in polycarbonate and polycarbonate/additive mixtures. *Colloid Polym. Sci.* **1987**, *265*, 815−822.
(31) Rössler, E.; Taupitz, M.; Börner, K.; Schulz, M.; Vieth, H. M. A simple method analyzing ^{2}H nuclear magnetic resonance line shapes to determine the activation energy distribution of mobile guest molecules in disordered systems. *J. Chem. Phys.* **1990**, *92*, 5847−5855.
(32) Grünberg, B.; Grünberg, A.; Limbach, H.-H.; Buntkowsky, G. Melting of naphthalene confined in mesoporous silica MCM-41. *Appl. Magn. Reson.* **2013**, *44*, 189−201.
(33) de Sousa Amadeu, N.; Grünberg, B.; Frydel, J.; Werner, M.; Limbach, H. H.; Breitzke, H.; Buntkowsky, G. Melting of low molecular weight compounds in confinement observed by ^{2}H-solid state NMR: Biphenyl, a case study. *Z. Phys. Chem.* **2012**, *226*, 1169−1186.
(34) Gedat, E.; Schreiber, A.; Albrecht, J.; Emmler, T.; Shenderovich, I.; Findenegg, G. H.; Limbach, H. H.; Buntkowsky, G. ^{2}H- solid state NMR study of benzene-d_6 confined in mesoporous silica SBA-15. *J. Phys. Chem. B* **2002**, *106*, 1977−1984.
(35) Kono, H.; Yunoki, S.; Shikano, T.; Fujiwara, M.; Erata, T.; Takai, M. CP/MAS ^{13}C NMR study of cellulose and cellulose Derivatives. 1. Complete assignment of the CP/MAS ^{13}C NMR spectrum of the native cellulose. *J. Am. Chem. Soc.* **2002**, *124*, 7506−7511.
(36) Goward, G. R.; Saalwächter, K.; Fischbach, I.; Spiess, H. W. Reorientation phenomena in imidazolium methyl sulfonate as probed by advanced solid-state NMR. *Solid State Nucl. Magn. Reson.* **2003**, *24*, 150−162.

https://dx.doi.org/10.1021/acs.jpcc.0c04905
J. Phys. Chem. C 2020, 124, 18886−18893